

Cosmological constraints from galaxy multi-tracers in the nearby Universe

Ginevra Favole*

*Institute of Cosmology & Gravitation, University of Portsmouth,
Dennis Sciama Building, Portsmouth, PO13FX, UK*

Domenico Sapone† and Javier Silva Lafaure‡

*Grupo de Cosmología y Astrofísica Teórica, Departamento de Física,
FCFM, Universidad de Chile, Blanco Encalada 2008, Santiago, Chile*

The Baryon Acoustic Oscillation (BAO) scale in the clustering of galaxies is a powerful standard ruler to measure cosmological distances and determine the geometry of the Universe. Past surveys have detected the BAO feature in the clustering of different galaxy samples, most of them composed of redder, quiescent galaxies and bluer, star-forming ones out to redshift $z \sim 1$. Besides these targets, new upcoming surveys will observe high-redshift galaxies with bright nebular emission lines out to $z \sim 2$, quasars and Lyman- α quasars at $z > 2$. All these different galaxy targets will be used as multi-tracers of the same underlying dark matter field. By combining them over wide cosmological volumes, we will be able to beat cosmic variance and measure the growth of structure with unprecedented accuracy. In this work, we measure the BAO scale in the two-point auto- and cross-correlation functions of three independent populations of multi-tracers extracted from the SDSS DR7 Main galaxy sample at redshift $0.02 < z < 0.22$. Combining their covariances, we find accurate constraints on the shift parameter $\alpha = 1.00 \pm 0.04$ and $D_V(z = 0.1)/r_s = 2.92 \pm 0.12$.

I. INTRODUCTION

During the last decades, observations have led to the general acceptance that the Universe is in a phase of accelerated expansion. In a homogeneous and isotropic Universe, the simplest way to account for such expansion is to introduce a constant term in the Einstein equations, dubbed as cosmological constant (Λ). Based on recent observations [1–3] and on the simplicity of the model, the cosmological constant is still the most accepted dark energy candidate responsible for the acceleration of the Universe. Despite of its simplicity, such a scenario has raised several theoretical issues, which have led cosmologists to invoke more sophisticated dark energy models without succeeding on the task, see [4]. An alternative approach suggests that we would need to modify the laws of gravity and make it weaker at larger scales to mimic, phenomenologically, the observed expansion [5, 6].

The fundamental observables that trace the dynamics of the Universe are the Hubble parameter $H(z)$ and the angular diameter distance $D_A(z)$, which are directly connected to the properties of matter and quantify the overall expansion of the Universe. Observational exploration is necessary to provide an indication about the dynamics of the Universe. One way of understanding this is to measure distances at different epochs. Modern cosmology has been revolutionised when the definition of *standard ruler* [7] was introduced: a distance scale in the Universe whose size and evolution with redshift are known. An ideal candidate is the Baryon Acoustic

Oscillation scale (BAO; [2]) observed at the last scattering surface in the Cosmic Microwave Background (CMB) radiation. This feature represents the width of the primordial density fluctuations that propagate as acoustic waves in the early baryon-photon fluid. Such a distance can be decomposed into a radial, $H(z)$, and a transverse, $D_A(z)$, direction, which allow us to measure the expansion history of the Universe. If the standard cosmological model, i.e. the structures that we see today, have been generated by gravitational collapse of the primordial seeds in an expanding, homogeneous and isotropic Universe, then we should see an excess of baryonic matter in the distribution of galaxies at the same comoving scale. This excess of baryonic matter is visible as a prominent peak around $110 h^{-1} \text{Mpc}$ in the galaxy two-point correlation function. The first detection of the BAO peak happened in SDSS [2] and was then confirmed by 2dFGRS [8], BOSS [9] and WiggleZ Dark Energy Survey [3], VIPERS [10] and eBOSS [11].

New upcoming surveys, such as the Dark Energy Spectroscopic Instrument (DESI) [12, 13], Euclid [14, 15], Subaru Prime Focus Spectrograph (PFS) [16, 17], the Large Synoptic Survey Telescope (LSST) [18], or the Wide Field Infrared Survey Telescope (WFIRST) [19, 20], will observe tens of hundreds of millions of galaxies positions and spectra covering enormous cosmological volumes and extend the observations at very high redshifts ($z \sim 2 - 3$). These observations will map the late time dynamics of the Universe with unprecedented precision (few percents on the final cosmological parameters [21]). It is therefore imperative to gain as much information as possible from these data sets.

One statistical limitation of measuring the cosmological parameters is due to the cosmic variance effects in the survey volume. Recently, it was shown [22, 23] that by cross-correlating different dark matter tracers over wide

*Electronic address: ginevra.favole@port.ac.uk

†Electronic address: domenico.sapone@uchile.cl

‡Electronic address: javier.silva@ug.uchile.cl

cosmological volumes it is possible to beat cosmic variance, dramatically reducing the uncertainties on the observables. In fact, while the effective volume still remains a limitation, the relative information between different species is not. In this paper, we show that using a multi-tracer approach we can lower the errors on the scale distortion parameter α . In particular, we use luminous red galaxies and emission line galaxies as tracers to map the dynamics of the Universe at $z \sim 0.1$.

The paper is organised as follow: in Section II, we describe the observational samples of multi-tracers used in the analysis; in Section III, we infer the measurements and observables considered; in Section IV, we explain the methodology used in the analysis. We conclude by presenting and discussing our main results in Section V.

II. DATA

We analyse three independent galaxy populations selected from the SDSS DR7 Main galaxy sample [24], each one composed of a different tracer, and all of them covering the redshift range $0.02 < z < 0.22$. Specifically, these samples are: two selections of emission line galaxies (ELGs), one of [O II] [25] and another one of H α emitters [26], plus a selection of luminous red galaxies (LRGs) [27]. These are the only galaxy multi-tracers currently available in the nearby Universe. The SDSS Main parent sample, which is brighter than $r = 17.77$, and covers an effective area of 7300 deg^2 [28], was extracted from the NYU-Value Added Galaxy Catalogue¹ [29] and it was spectroscopically matched (i.e. matching the redshifts) to the MPA-JHU² DR7 release of spectral measurements to assign emission line properties.

We consider only ELGs with well measured spectra, i.e. those with the flag ZWARNING=0, and with good signal-to-noise, i.e. $S/N > 5$. Both [O II] and H α ELG samples have specific star formation rate of $\log(\text{sSFR}/\text{M}_{\odot}\text{yr}^{-1}) > -11$ and line equivalent width of $\text{EW} > 10 \text{ \AA}$ to guarantee that we are selecting only very star-forming galaxies. In addition, they are both limited in flux at $2 \times 10^{-16} \text{ erg cm}^{-2} \text{ s}^{-1}$ to match the Euclid nominal expected depth and flux limit [30] at higher redshift. The LRG sample includes only galaxies with $\log(\text{sSFR}/\text{M}_{\odot}\text{yr}^{-1}) < -11$, which are all quiescent.

The observed (i.e. attenuated by dust) [O II] and H α ELG luminosities are computed from the corresponding flux densities F as:

$$L [\text{erg s}^{-1}] = 4\pi D_L^2 10^{-0.4(r_p - r_{\text{fib}})} F, \quad (1)$$

where D_L is the luminosity distance as a function of cosmology and the exponent is the SDSS fibre aperture correction written in terms of the r -band petrosian and fibre

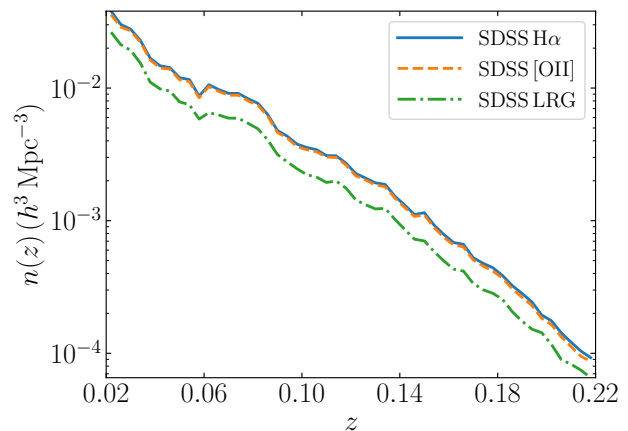


FIG. 1: Galaxy number density, as a function of redshift, of the SDSS H α , [O II] and LRG samples at $0.02 < z < 0.22$.

magnitudes. For further details on the luminosity calculations, we refer the reader to [25, 26].

Fig. 1 shows the galaxy number density of the SDSS H α , [O II] and LRG samples as a function of redshift. Compared to the SDSS Main sample in [31], our galaxy selections cover a larger area (we consider both North and South Galactic Caps) and span a slightly different redshift range. Therefore, it is not surprising that our galaxy number densities differ from [31]. In particular, our $n(z)$ values are large enough to ensure that the SDSS H α , [O II] and LRG samples are limited by cosmic variance (i.e., $n(z)P(k) > 1$) at $z < 0.22$ for $k < 0.095, 0.093, 0.071 h \text{ Mpc}^{-1}$, respectively.

III. MEASUREMENTS

In Large Scale Structure (LSS) analysis, galaxies can be thought as point-like objects in space-time that move along with the expansion of the Universe, forming bounded structures due to their gravitational interaction. By analysing their positions, we can gain information on the underlying theory of gravity. One method consists in quantifying how many objects are present in a given cosmological volume. This method relies on the two-point correlation function (2PCF), which is the excess probability over randoms of finding two galaxies separated by a distance s in redshift-space.

We measure the two-point auto- and cross-correlation functions of the three galaxy tracers defined in Sec. II using the Landy and Szalay estimator:

$$\xi_{\mu\nu}(s) = \frac{D_\mu D_\nu(s) - D_\mu R_\nu(s) - D_\nu R_\mu(s)}{R_\mu R_\nu(s)} + 1, \quad (2)$$

where $s = \sqrt{\pi^2 + r_p^2}$ represents the redshift-space distance as a function of the parallel (π) and perpendicular (r_p) components to the line of sight, while μ and

¹ <http://cosmo.nyu.edu/blanton/vagc/>

² <http://www.mppg.de/SDSS/DR7/>

ν are the tracers. The DD, DR and RR terms are the normalised and weighted data-data, data-random and random-random pair counts formed from the observed galaxies and the synthetic randoms. We use the equal surface density randoms from the NYU-VAGC. The weighting scheme adopted for the pair counts is $w = w_{\text{fc}} w_{\text{ang}} w_{\text{FKP}}$ for data and $w = w_{\text{FKP}}$ for randoms. The w_{fc} term represents the fibre collision weight (in SDSS fibres cannot be placed closer than $55''$). The angular weight $w_{\text{ang}} = 1/f_{\text{got}}$ accounts for the angular sector completeness, and the FKP [32] one,

$$w_{\text{FKP}} = \frac{1}{1 + \bar{n}(z)P_0}, \quad (3)$$

corrects for any fluctuation in the number density of tracers. In Eq. (3), $\bar{n}(z)$ is the expected number density of a galaxy at redshift z and we set $P_0 = 16000 h^{-3} \text{Mpc}^3$, which is close to the amplitude of the SDSS power spectrum at $k = 0.1 h \text{Mpc}^{-1}$ [31].

We estimate the uncertainties on the SDSS clustering measurements via 200 jackknife re-samplings [33–37] containing about the same number of data (randoms) each. The covariance matrix for each 2PCF is calculated as [34, 37, 38]:

$$\hat{C}_{ij} = \frac{N_{\text{res}} - 1}{N_{\text{res}}} \sum_{a=1}^{N_{\text{res}}} (\xi_i^a - \bar{\xi}_i^a)(\xi_j^a - \bar{\xi}_j^a), \quad (4)$$

where the pre-factor takes into account that in every re-sampling $N_{\text{res}} - 2$ sub-volumes are the same [35], and $\bar{\xi}_i$ is the mean jackknife correlation function in the i^{th} bin:

$$\bar{\xi}_i = \sum_{a=1}^{N_{\text{res}}} \xi_i^a / N_{\text{res}}. \quad (5)$$

The full covariance matrix for all the tracers is built by combining the individual ones in Eq. (4) as:

$$\hat{C} = \begin{pmatrix} \hat{C}_{\text{H}\alpha-\text{H}\alpha} & \hat{C}_{\text{H}\alpha-[\text{OII}]} & \hat{C}_{\text{H}\alpha-\text{LRG}} \\ \hat{C}_{\text{H}\alpha-[\text{OII}]} & \hat{C}_{[\text{OII}]-[\text{OII}]} & \hat{C}_{[\text{OII}]-\text{LRG}} \\ \hat{C}_{\text{H}\alpha-\text{LRG}} & \hat{C}_{[\text{OII}]-\text{LRG}} & \hat{C}_{\text{LRG}-\text{LRG}} \end{pmatrix}. \quad (6)$$

The inverse of the covariance matrix, the so-called “precision matrix” $\hat{\Psi} \equiv \hat{C}^{-1}$, requires some corrections. In fact, Eq. (6) is obtained from a limited set of re-samplings, N_{res} , and it has an associated error which propagates into the precision matrix. Following [39], we implement two corrections to obtain an unbiased estimate of the precision matrix and to reduce the noise in its off-diagonal terms. The bias correction consists in multiplying \hat{C}^{-1} by the Hartlap factor [40], which accounts for the limited number of re-samplings and the number of bins n_b in our measurements of ξ :

$$\hat{\Psi} = \left(1 - \frac{n_b + 1}{N_{\text{res}} - 1}\right) \hat{C}^{-1}, \quad (7)$$

The noise correction, also known as “covariance taper-

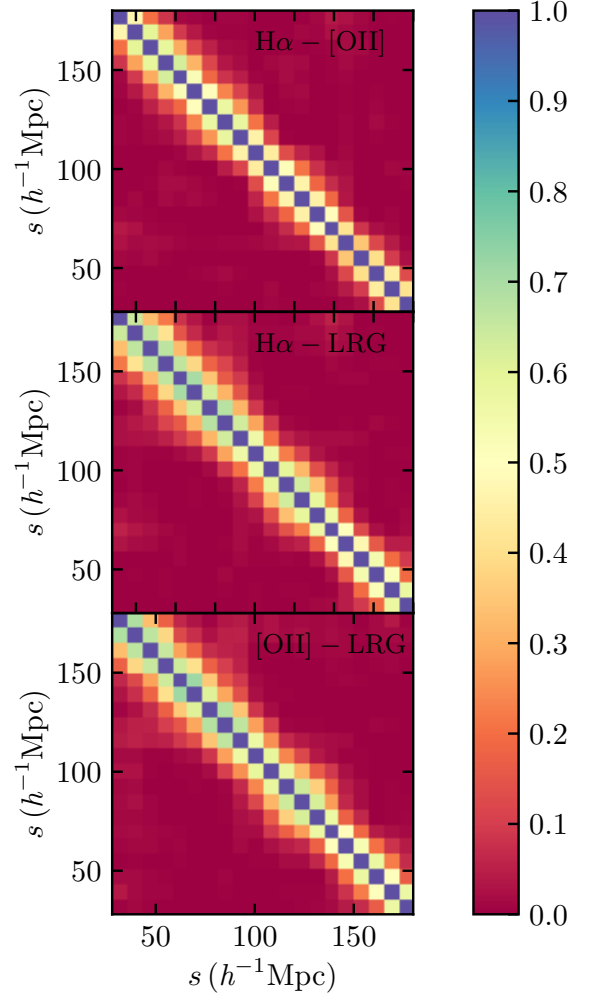


FIG. 2: Normalised covariance matrices obtained from the monopole cross-correlation functions of the SDSS galaxy tracers. From top to bottom: $\text{H}\alpha$ -[OII], $\text{H}\alpha$ -LRG and [OII]-LRG.

ing” [41], can be applied to both covariance and precision matrices. The idea of this method is to neglect the correlation between data pairs far apart through a kernel function of the Matérn class. Such a correction relies on the tapering matrix $T_{ij} \equiv K(|s_i - s_j|)$, which is defined as a monoparametric Kernel function [39, 42, 43] depending on the physical scale of the tracers that we are correlating. This kernel also includes a tapering parameter T_p , which identifies the interval where $K(x)$ takes non-zero values, guaranteeing a vanishing correlation between pairs for larger distances. The final corrected precision matrix is:

$$\hat{\Psi} = \left(1 - \frac{n_b + 1}{N_{\text{res}} - 1}\right) (\hat{C} \circ T)^{-1} \circ T, \quad (8)$$

where the \circ symbol indicates the Hadamard product. In our analysis, we assume a tapering parameter $T_p = 50 h^{-1} \text{Mpc}$ to ensure that the entire covariance matrix is positive semi-definite. Fig. 2 shows the normalised

covariance matrices obtained from the monopole cross-correlation functions of the SDSS H α -[O II], H α -LRG and [O II]-LRG multi-tracers.

IV. METHODOLOGY

The real-space two-point correlation function $\xi(r)$ is the spatially isotropic Fourier transform of the matter power spectrum $P(k)$ defined as:

$$\xi(r) = \frac{1}{2\pi^2} \int P(k) \frac{\sin(kr)}{kr} k^2 dk. \quad (9)$$

The position of the BAO peak inferred from Eq. (9) is expected to appear around $110 h^{-1} \text{Mpc}$, which is well beyond the scales of virialised objects. This implies that the non-linear gravitational effects can be safely ignored. For the power spectrum we use the template [44]:

$$P(k) = [P_{\text{lin}}(k) - P_{\text{dw}}(k)] e^{-k^2 \Sigma_{\text{nl}}^2/2} + P_{\text{dw}}(k), \quad (10)$$

where $P_{\text{lin}}(k)$ is the linear matter power spectrum calculated using the Boltzmann code CLASS [45], and $P_{\text{dw}}(k)$ is the de-wiggled power spectrum [46], both using Planck 2015 [47] fiducial cosmology. The Σ_{nl} parameter accounts for the smoothing of the BAO peak due to non-linear effects [48].

We compute the theoretical correlation functions needed to fit the SDSS multi-tracer measurements by applying Eq. (9) with the power spectrum given in Eq. (10). We model the BAO signal as [49]:

$$\xi_{\text{model}}(s) = B\xi(\alpha s) + a_0 + \frac{a_1}{s} + \frac{a_2}{s^2}, \quad (11)$$

where a_1, a_2, a_3 are linear nuisance parameters and B accounts for all possible effects on the clustering amplitude, such as the linear bias, the normalisation of the power spectrum, σ_8 , and the redshift space distortions [49]. In addition, we introduce the shift parameter α which takes into account the distortion between distances measured in the data due to the fiducial cosmology chosen to build the estimator. This is defined as [44]:

$$\alpha = \frac{D_V}{r_s} \frac{r_s^{\text{fid}}}{D_V^{\text{fid}}}, \quad (12)$$

where r_s represents the sound-horizon [46, 50] and D_V is the volume-averaged distance defined as [2]:

$$D_V(z) = [cz(1+z)^2 D_A^2(z) H^{-1}(z)]^{1/3}, \quad (13)$$

where $D_A(z)$ and $H(z)$ are the angular diameter distance and the Hubble parameter at redshift z , respectively.

We use a Monte Carlo Markov Chain (MCMC) based on a Metropolis-Hastings algorithm³ to find the optimal

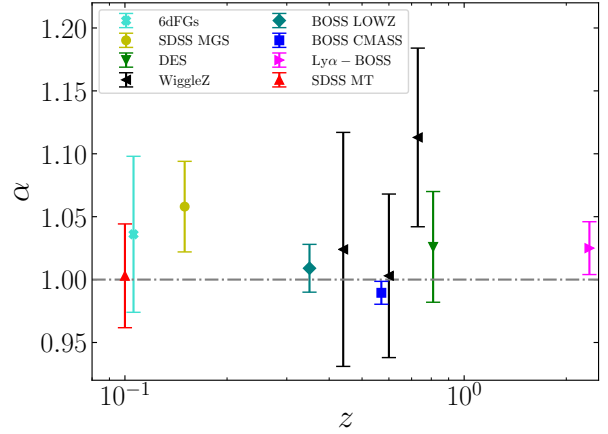


FIG. 3: Shift parameter α as a function of redshift from different BAO measurements: 6dFGs [51], MGS [31], DES [52], WiggleZ [3], Lowz-BOSS [53], CMASS-BOSS [49] and Ly α -BOSS [54]

parameter values. We assume a likelihood function of the form $\mathcal{L} \propto \exp(-\chi^2/2)$, where the χ^2 is computed as:

$$\chi^2(\alpha, B) = (\vec{\xi}_{\text{model}} - \vec{\xi}_{\text{obs}})^T \hat{\Psi} (\vec{\xi}_{\text{model}} - \vec{\xi}_{\text{obs}}). \quad (14)$$

In the equation above, $\vec{\xi}_{\text{model}}$ is the theoretical correlation function given in Eq. (11), $\vec{\xi}_{\text{obs}}$ is the observed one, both grouped in a vector at each position, and $\hat{\Psi}$ is the precision matrix given in Eq. (8).

V. RESULTS AND DISCUSSIONS

In this analysis, we have considered different model scenarios with an increasing level of complexity. Our main results are summarised in Tab. I and shown in Fig. 3, together with previous results from literature. First, we use the model given in Eq. (11), which has 5 parameters (5p) common to all the targets: $(B, \alpha, a_0, a_1, a_2)$. This is equivalent to assume that all the targets respond in the same way to the gravitational interaction and expansion. The second model we test is a modification of Eq. (11), with 13 independent parameters (13p): α , common to all the targets, plus three different sets of (B, a_0, a_1, a_2) . The last model used is again a modification of Eq. (11), with three different sets of $(B, \alpha, a_0, a_1, a_2)$ i.e., 15 parameters (15p) in total. As a test, we also report the analysis performed using only LRG target. In the 5p scenario, we find a shift parameter of $\alpha = 1.00 \pm 0.04$, while in the 13p model $\alpha = 1.01 \pm 0.04$. In the 15p scenario, we find $\alpha = 1.02 \pm 0.04$ for both H α and [O II], and $\alpha = 0.97 \pm 0.05$ for LRGs. The latter is consistent with $\alpha = 0.96 \pm 0.07$ found using only LRGs, which is directly comparable to the results at $z \sim 0.15$ by [31] and at $z \sim 0.35$ by [55].

³ <https://emcee.readthedocs.io/en/stable/>

Models:	5p	13p	15p	LRG
$\alpha_{H\alpha}$	-	-	$1.02^{0.04}_{0.03}$	-
α_{OII}	-	-	$1.02^{0.04}_{0.04}$	-
α_{LRG}	-	-	$0.97^{0.05}_{0.05}$	$0.96^{0.07}_{0.06}$
α	$1.00^{0.04}_{0.04}$	$1.01^{0.04}_{0.04}$	-	-

TABLE I: Best-fit constraints from our models.

For our fiducial cosmology, we find a volume-averaged distance of $D_V^{\text{fid}}(z = 0.1) = 429.90 \text{ Mpc}$, and $D_V^{\text{fid}}(z = 0.1)/r_s^{\text{fid}} = 2.92$. By combining Eq. (12) with the constraints obtained on α , we find that the 1σ uncertainty on D_V/r_s is ~ 0.12 . Assuming $r_s = 147.41 \text{ Mpc}$ [47], we find $D_V = (435.07 \pm 17.14) \text{ Mpc}$.

Our study relies on the jackknife covariance matrices from SDSS data, corrected from bias and noise (see Sec. III), whereas [31] use covariances from synthetic mock catalogues. As shown by [34] and [56], jackknife returns reliable covariance estimates only on large scales, that are the scales of interest in our cosmological analysis. Hence, we do not expect our results to change substantially if covariance matrices from mocks were used.

Another difference between our analysis and [31] is the fact that we do not reconstruct the density field. The main idea of BAO reconstruction [57, 58] is to smooth the linear matter density field and to sharpen the acoustic peak in the correlation function. This method has the advantage of accurately constraining the non-linear parameter Σ_{nl} . In our analysis we find $\Sigma_{\text{nl}} \sim 20 \text{ Mpc } h^{-1}$, while [31] find $\Sigma_{\text{nl}} \sim 5 \text{ Mpc } h^{-1}$. A lower value of Σ_{nl} provides a better signal and tighter constraints on both B and α . Our results are fairly compared and in agreement within 1σ with the pre-reconstruction value of $\alpha = 1.01 \pm 0.09$ from [31] for LRGs only. The uncertainty we find on α

using our multi-tracer analysis is 0.04, identical to the post-reconstruction estimate by [31], and 44% smaller than their pre-reconstruction value. Hence, we expect that by implementing reconstruction on mocks for galaxy multi-tracers, we will be able to significantly reduce our current error. This result highlights the great potentiality of combining different tracers to constrain more accurately the cosmological parameters.

We remind the reader that for all the models used in this work we assumed flat priors, differently from [31], where Gaussian priors are considered. Flat priors are less informative, but they do not rule out any region of the parameter space.

We have performed a cosmological analysis on the LRG, $H\alpha$ and $[OII]$ ELG multi-tracers currently available at $z \sim 0.1$. For the future, we plan to extend the multi-tracer methodology tested here to the upcoming data sets from the new spectroscopic surveys, such as DESI or Euclid. Our ultimate goal is to include synthetic mock catalogues for galaxy multi-tracers testing the impact of BAO reconstruction on our results. This will enable us to improve the multi-tracer covariance estimates on all scales, and hopefully we will be able to put tight constraints on the non-linear redshift-space distortions.

VI. ACKNOWLEDGMENTS

GF is funded through a Dennis Sciama fellowship at the Institute of Cosmology and Gravitation (ICG), at Portsmouth University. JS acknowledges financial support from CONICYT. The authors are grateful to Melita Carbone and Philipp Sudek for insightful discussions and to Daniel Eisenstein for providing useful comments during the preparation of this work.

-
- [1] **Planck** Collaboration, N. Aghanim *et al.*, “Planck 2018 results. VI. Cosmological parameters,” [arXiv:1807.06209 \[astro-ph.CO\]](#).
 - [2] **SDSS** Collaboration, D. J. Eisenstein *et al.*, “Detection of the Baryon Acoustic Peak in the Large-Scale Correlation Function of SDSS Luminous Red Galaxies,” *Astrophys. J.* **633** (2005) 560–574, [arXiv:astro-ph/0501171 \[astro-ph\]](#).
 - [3] C. Blake *et al.*, “The WiggleZ Dark Energy Survey: testing the cosmological model with baryon acoustic oscillations at $z=0.6$,” *Mon. Not. Roy. Astron. Soc.* **415** (2011) 2892–2909, [arXiv:1105.2862 \[astro-ph.CO\]](#).
 - [4] D. Sapone, “Dark Energy in Practice,” *Int. J. Mod. Phys. A* **25** (2010) 5253–5331, [arXiv:1006.5694 \[astro-ph.CO\]](#).
 - [5] M. Kunz and D. Sapone, “Dark Energy versus Modified Gravity,” *Phys. Rev. Lett.* **98** (2007) 121301, [arXiv:astro-ph/0612452 \[astro-ph\]](#).
 - [6] S. Tsujikawa, “Modified gravity models of dark energy,” *Lect. Notes Phys.* **800** (2010) 99–145, [arXiv:1101.0191 \[gr-qc\]](#).
 - [7] H.-J. Seo and D. J. Eisenstein, “Probing dark energy with baryonic acoustic oscillations from future large galaxy redshift surveys,” *Astrophys. J.* **598** (2003) 720–740, [arXiv:astro-ph/0307460 \[astro-ph\]](#).
 - [8] **2dFGRS** Collaboration, S. Cole *et al.*, “The 2dF Galaxy Redshift Survey: Power-spectrum analysis of the final dataset and cosmological implications,” *Mon. Not. Roy. Astron. Soc.* **362** (2005) 505–534, [arXiv:astro-ph/0501174 \[astro-ph\]](#).
 - [9] **BOSS** Collaboration, K. S. Dawson *et al.*, “The Baryon Oscillation Spectroscopic Survey of SDSS-III,” *Astron. J.* **145** (2013) 10, [arXiv:1208.0022 \[astro-ph.CO\]](#).
 - [10] S. de la Torre *et al.*, “The VIMOS Public Extragalactic Redshift Survey (VIPERS). Galaxy clustering and redshift-space distortions at $z=0.8$ in the first data release,” *Astron. Astrophys.* **557** (2013) A54, [arXiv:1303.2622 \[astro-ph.CO\]](#).
 - [11] K. S. Dawson *et al.*, “The SDSS-IV extended Baryon Oscillation Spectroscopic Survey: Overview and Early

- Data,” *Astron. J.* **151** (2016) 44, arXiv:1508.04473 [astro-ph.CO].
- [12] **DESI** Collaboration, A. Aghamousa *et al.*, “The DESI Experiment Part I: Science, Targeting, and Survey Design,” arXiv:1611.00036 [astro-ph.IM].
- [13] **DESI** Collaboration, A. Aghamousa *et al.*, “The DESI Experiment Part II: Instrument Design,” arXiv:1611.00037 [astro-ph.IM].
- [14] **EUCLID** Collaboration, R. Laureijs *et al.*, “Euclid Definition Study Report,” arXiv:1110.3193 [astro-ph.CO].
- [15] L. Amendola *et al.*, “Cosmology and fundamental physics with the Euclid satellite,” *Living Rev. Rel.* **21** no. 1, (2018) 2, arXiv:1606.00180 [astro-ph.CO].
- [16] H. Sugai *et al.*, “Prime focus spectrograph: Subaru’s future,” *Proc. SPIE Int. Soc. Opt. Eng.* **8446** (2012) 84460Y, arXiv:1210.2719 [astro-ph.IM].
- [17] S. Smee *et al.*, “The Multi-Object, Fiber-Fed Spectrographs for SDSS and the Baryon Oscillation Spectroscopic Survey,” *Astron. J.* **146** (2013) 32, arXiv:1208.2233 [astro-ph.IM].
- [18] **LSST Science, LSST Project** Collaboration, P. A. Abell *et al.*, “LSST Science Book, Version 2.0,” arXiv:0912.0201 [astro-ph.IM].
- [19] J. Green *et al.*, “Wide-Field InfraRed Survey Telescope (WFIRST) Final Report,” arXiv:1208.4012 [astro-ph.IM].
- [20] D. Spergel *et al.*, “Wide-Field InfrarRed Survey Telescope-Astrophysics Focused Telescope Assets WFIRST-AFTA 2015 Report,” arXiv:1503.03757 [astro-ph.IM].
- [21] **Euclid** Collaboration, A. Blanchard *et al.*, “Euclid preparation: VII. Forecast validation for Euclid cosmological probes,” arXiv:1910.09273 [astro-ph.CO].
- [22] L. R. Abramo and K. E. Leonard, “Why multi-tracer surveys beat cosmic variance,” *Mon. Not. Roy. Astron. Soc.* **432** (2013) 318, arXiv:1302.5444 [astro-ph.CO].
- [23] A. D. Montero-Dorta, L. R. Abramo, B. R. Granett, S. de la Torre, and L. Guzzo, “The Multi-Tracer Optimal Estimator applied to VIPERS,” arXiv:1909.00010 [astro-ph.CO].
- [24] **SDSS** Collaboration, M. A. Strauss *et al.*, “Spectroscopic Target Selection in the Sloan Digital Sky Survey: The Main Galaxy Sample,” *Astron. J.* **124** (2002) 1810, arXiv:astro-ph/0206225 [astro-ph].
- [25] G. Favole, S. A. Rodríguez-Torres, J. Comparat, F. Prada, H. Guo, A. Klypin, and A. D. Montero-Dorta, “Galaxy clustering dependence on the [O II] emission line luminosity in the local universe,” *Monthly Notices of the Royal Astronomical Society* **472** no. 1, (Aug, 2017) 550–558.
- [26] G. Favole, “The clustering of H α emitters in the nearby Universe,” *in preparation* (2019) .
- [27] **SDSS** Collaboration, D. J. Eisenstein *et al.*, “Spectroscopic target selection for the Sloan Digital Sky Survey: The Luminous red galaxy sample,” *Astron. J.* **122** (2001) 2267, arXiv:astro-ph/0108153 [astro-ph].
- [28] H. Guo *et al.*, “Redshift-space clustering of SDSS galaxies - luminosity dependence, halo occupation distribution, and velocity bias,” *Mon. Not. Roy. Astron. Soc.* **453** no. 4, (2015) 4368–4383, arXiv:1505.07861 [astro-ph.CO].
- [29] **SDSS** Collaboration, M. R. Blanton *et al.*, “NYU-VAGC: A Galaxy catalog based on new public surveys,” *Astron. J.* **129** (2005) 2562–2578, arXiv:astro-ph/0410166 [astro-ph].
- [30] A. Merson, Y. Wang, A. Benson, A. Faisst, D. Masters, A. Kiessling, and J. Rhodes, “Predicting H α emission-line galaxy counts for future galaxy redshift surveys,” *Mon. Not. Roy. Astron. Soc.* **474** no. 1, (2018) 177–196, arXiv:1710.00833 [astro-ph.GA].
- [31] A. J. Ross, L. Samushia, C. Howlett, W. J. Percival, A. Burden, and M. Manera, “The clustering of the SDSS DR7 main Galaxy sample ? I. A 4 per cent distance measure at $z = 0.15$,” *Mon. Not. Roy. Astron. Soc.* **449** no. 1, (2015) 835–847, arXiv:1409.3242 [astro-ph.CO].
- [32] H. A. Feldman, N. Kaiser, and J. A. Peacock, “Power spectrum analysis of three-dimensional redshift surveys,” *Astrophys. J.* **426** (1994) 23–37, arXiv:astro-ph/9304022 [astro-ph].
- [33] L. D. Miller, M. E. Miller, and M. Sivvy, “The jackknife-a review,” *Biometrika* (1974) 1–15.
- [34] P. Norberg, C. M. Baugh, E. Gaztanaga, and D. J. Croton, “Statistical Analysis of Galaxy Surveys - I. Robust error estimation for 2-point clustering statistics,” *Mon. Not. Roy. Astron. Soc.* **396** (2009) 19, arXiv:0810.1885 [astro-ph].
- [35] P. Norberg, E. Gaztanaga, C. M. Baugh, and D. J. Croton, “Statistical Analysis of Galaxy Surveys-IV: An objective way to quantify the impact of superstructures on galaxy clustering statistics,” *Mon. Not. Roy. Astron. Soc.* **418** (2011) 2435, arXiv:1106.5701 [astro-ph.CO].
- [36] H. Guo *et al.*, “The clustering of galaxies in the SDSS-III Baryon Oscillation Spectroscopic Survey: Luminosity and Color Dependence and Redshift Evolution,” *Astrophys. J.* **767** (2013) 122, arXiv:1212.1211 [astro-ph.CO].
- [37] G. Favole, C. K. McBride, D. J. Eisenstein, F. Prada, M. E. Swanson, C.-H. Chuang, and D. P. Schneider, “Building a better understanding of the massive high-redshift BOSS CMASS galaxies as tools for cosmology,” *Mon. Not. Roy. Astron. Soc.* **462** no. 2, (2016) 2218–2236, arXiv:1506.02044 [astro-ph.CO].
- [38] B. Efron, *The Jackknife, the Bootstrap and other resampling plans*. 1982.
- [39] D. J. Paz and A. G. Sanchez, “Improving the precision matrix for precision cosmology,” *Mon. Not. Roy. Astron. Soc.* **454** no. 4, (2015) 4326–4334, arXiv:1508.03162 [astro-ph.CO].
- [40] J. Hartlap, P. Simon, and P. Schneider, “Why your model parameter confidences might be too optimistic: Unbiased estimation of the inverse covariance matrix,” *Astron. Astrophys.* (2006) , arXiv:astro-ph/0608064 [astro-ph]. [Astron. Astrophys. **464**, 399 (2007)].
- [41] C. G. Kaufman, M. J. Schervish, and D. W. Nychka, “Covariance tapering for likelihood-based estimation in large spatial data sets,” *Journal of the American Statistical Association* **103** no. 484, (2008) 1545–1555.
- [42] H. Wendland, “Piecewise polynomial, positive definite and compactly supported radial functions of minimal degree,” *Advances in Computational Mathematics* **4** no. 1, (Dec, 1995) 389–396.
- [43] H. Wendland, “Error estimates for interpolation by compactly supported radial basis functions of minimal

- degree,” *Journal of Approximation Theory* **93** no. 2, (1998) 258 – 272.
- [44] N. Padmanabhan and M. J. White, “Constraining Anisotropic Baryon Oscillations,” *Phys. Rev.* **D77** (2008) 123540, arXiv:0804.0799 [astro-ph].
- [45] J. Lesgourgues, “The Cosmic Linear Anisotropy Solving System (CLASS) I: Overview,” arXiv:1104.2932 [astro-ph.IM].
- [46] D. J. Eisenstein and W. Hu, “Baryonic features in the matter transfer function,” *Astrophys. J.* **496** (1998) 605, arXiv:astro-ph/9709112 [astro-ph].
- [47] **Planck** Collaboration, P. A. R. Ade *et al.*, “Planck 2015 results. XIII. Cosmological parameters,” *Astron. Astrophys.* **594** (2016) A13, arXiv:1502.01589 [astro-ph.CO].
- [48] M. Crocce and R. Scoccimarro, “Renormalized cosmological perturbation theory,” *Phys. Rev.* **D73** (2006) 063519, arXiv:astro-ph/0509418 [astro-ph].
- [49] X. Xu, N. Padmanabhan, D. J. Eisenstein, K. T. Mehta, and A. J. Cuesta, “A 2% Distance to $z=0.35$ by Reconstructing Baryon Acoustic Oscillations - II: Fitting Techniques,” *Mon. Not. Roy. Astron. Soc.* **427** (2012) 2146, arXiv:1202.0091 [astro-ph.CO].
- [50] W. Hu and N. Sugiyama, “Small scale cosmological perturbations: An Analytic approach,” *Astrophys. J.* **471** (1996) 542–570, arXiv:astro-ph/9510117 [astro-ph].
- [51] F. Beutler, C. Blake, M. Colless, D. H. Jones, L. Staveley-Smith, L. Campbell, Q. Parker, W. Saunders, and F. Watson, “The 6dF Galaxy Survey: Baryon Acoustic Oscillations and the Local Hubble Constant,” *Mon. Not. Roy. Astron. Soc.* **416** (2011) 3017–3032, arXiv:1106.3366 [astro-ph.CO].
- [52] **DES** Collaboration, T. M. C. Abbott *et al.*, “Dark Energy Survey Year 1 Results: Measurement of the Baryon Acoustic Oscillation scale in the distribution of galaxies to redshift 1,” *Mon. Not. Roy. Astron. Soc.* **483** no. 4, (2019) 4866–4883, arXiv:1712.06209 [astro-ph.CO].
- [53] H. Gil-Marn *et al.*, “The clustering of galaxies in the SDSS-III Baryon Oscillation Spectroscopic Survey: BAO measurement from the LOS-dependent power spectrum of DR12 BOSS galaxies,” *Mon. Not. Roy. Astron. Soc.* **460** no. 4, (2016) 4210–4219, arXiv:1509.06373 [astro-ph.CO].
- [54] **BOSS** Collaboration, T. Delubac *et al.*, “Baryon acoustic oscillations in the Ly α forest of BOSS DR11 quasars,” *Astron. Astrophys.* **574** (2015) A59, arXiv:1404.1801 [astro-ph.CO].
- [55] C.-H. Chuang and Y. Wang, “Measurements of $H(z)$ and $DA(z)$ from the two-dimensional two-point correlation function of Sloan Digital Sky Survey luminous red galaxies,” *Monthly Notices of the Royal Astronomical Society* **426** no. 1, (10, 2012) 226–236.
- [56] O. H. E. Philcox, D. J. Eisenstein, R. O’Connell, and A. Wiegand, “RascalC: A Jackknife Approach to Estimating Single and Multi-Tracer Galaxy Covariance Matrices,” arXiv:1904.11070 [astro-ph.CO].
- [57] D. J. Eisenstein, H.-j. Seo, E. Sirko, and D. Spergel, “Improving Cosmological Distance Measurements by Reconstruction of the Baryon Acoustic Peak,” *Astrophys. J.* **664** (2007) 675–679, arXiv:astro-ph/0604362 [astro-ph].
- [58] N. Padmanabhan, X. Xu, D. J. Eisenstein, R. Scalzo, A. J. Cuesta, K. T. Mehta, and E. Kazin, “A 2 per cent distance to $z=0.35$ by reconstructing baryon acoustic oscillations - I. Methods and application to the Sloan Digital Sky Survey,” *Mon. Not. Roy. Astron. Soc.* **427** no. 3, (2012) 2132–2145, arXiv:1202.0090 [astro-ph.CO].